

# Interference and nuclear medium effects on the eta-mesic nuclear spectrum

Q. Haider\*

*Physics Department, Fordham University  
Bronx, N.Y. 10458, USA*

Lon-chang (L.C.) Liu†

*Theoretical Division, Group T-2, Mail Stop B214  
Los Alamos National Laboratory, Los Alamos, N.M. 87545, USA*

(Dated: September 30, 2010)

## Abstract

The missing-mass spectrum obtained in a recoil-free transfer reaction  $p(^{27}\text{Al}, ^3\text{He})\pi^- p'X$  is analyzed. We find that the observed peak structure arises from the coherent contributions from two reaction processes in the energy region corresponding to a bound eta ( $\eta$ ) meson. In one of the processes the intermediate  $\eta$  is captured by the nucleus to form the  $\eta$ -mesic nucleus  $^{25}\text{Mg}_\eta$ . In the other process, the  $\eta$  does not form  $\eta$ -nucleus bound state. The interference between these two processes has caused the peak of the spectrum to appear at an  $\eta$  binding energy stronger than the actual one. Our analysis also indicates that the data are consistent with an attractive  $N^*(1535)$ -nucleus interaction at energies below the  $\eta N$  threshold.

Keywords: Nuclear interaction of  $N^*(1535)$ , Eta-mesic nucleus  $^{25}\text{Mg}_\eta$ .

PACS Numbers: 24.10.Eq, 24.10.-i, 21.10.Dr

---

\* e-mail address: haider@fordham.edu

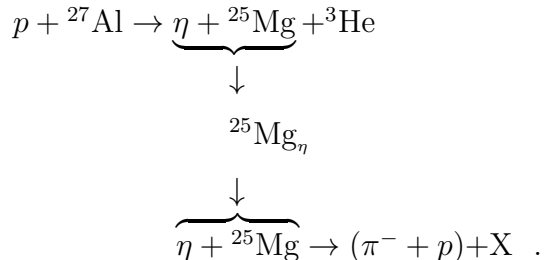
† e-mail address: liu@lanl.gov

## I. INTRODUCTION

The possibility of an eta ( $\eta$ ) meson being bound in a nucleus by strong-interaction force, leading to the formation of an exotic nucleus called eta-mesic nucleus, was first proposed in 1986 [1]. The nuclear binding of an  $\eta$  meson is caused by an attractive eta-nucleon ( $\eta$ N) interaction in the threshold region. This attractive  $\eta$ N interaction is due to the  $N^*(1535)$  resonance being situated not too far above the threshold of the  $\eta$ N channel (1488 MeV). It was also shown in Ref.[1] that a bound state is possible if there is a sufficient number of nucleons (10 or more) in a nucleus.

The existence of  $\eta$ -mesic nuclei will certainly create new premises for studying  $\eta$  meson and baryon resonances inside nuclei. Extensive interest in exploring this new venue is evidenced by the large amount of theoretical work that has been done during the last two decades [2]-[16]. Irrespective of the models and formalisms used, from a theoretical point of view there is unanimity about the existence of  $\eta$ -mesic nucleus.

Recently, the COSY-GEM collaboration [17] searched for  $\eta$ -mesic nucleus by means of a recoil-free transfer reaction  $p(^{27}\text{Al}, ^3\text{He})\pi^-p'X$ . The kinematics was so chosen that the  $\eta$  produced in the intermediate state is nearly at rest, favoring its capture by the residual nucleus  $^{25}\text{Mg}$ . Because of energy conservation, the bound  $\eta$  cannot reappear as an observable particle in the decay products of the mesic nucleus  $^{25}\text{Mg}_\eta$ . Instead, it interacts, for example, with a target neutron resulting in the emission of a nearly “back-to-back”  $\pi^-p$  pair in the laboratory. We denote this multi-step reaction as Process M (M for mesic-nucleus):



In order to reduce a large number of background events arising from particles being emitted during nuclear cascade process, the COSY-GEM collaboration implemented a triple-coincidence measurement among  $^3\text{He}$  and the “back-to-back”  $\pi^-p$  pair having the kinetic energy spectra of the pion and proton peaked, respectively, at about 100 and 320 MeV [18].

Because of this background reduction, a peak in the missing-mass spectrum in the energy region corresponding to bound  $\eta$  has been made evident. Upon fitting the spectrum with the sum of a background term and a Gaussian ( $|f_b|^2 + |f_g|^2$ ), COSY-GEM collaboration determined that the peak has its centroid situated at binding energy ( $-13.13 \pm 1.64$ ) MeV with a FWHM of ( $10.22 \pm 2.98$ ) MeV [or a half-width  $\Gamma/2 \simeq (5.1 \pm 1.5)$  MeV].

By performing a bound-state calculation based on scattering length and using on-shell kinematics, we find that the above binding energy and half-width correspond to an effective  $s$ -wave  $\eta$ N scattering length  $a_0 \simeq (0.292 + 0.077i)$  fm. An exceptional feature of this scattering length is its imaginary-to-real part ratio  $R \equiv \mathcal{I}m(a_0)/\mathcal{R}e(a_0) = 0.26$  only, while most of the published theoretical models give scattering lengths (see table I of Ref.[19]) having  $R \gg 0.35$ . In other words, the value of  $R$  given by the theories is higher than the fitted value by at least 35%. The need to understand the huge difference between theory and experiment has motivated the present study.

More specifically, we will reanalyze the experiment and infer from our analysis the nature of the observed peak structure and the qualitative feature of the  $N^*(1535)$ -nucleus interaction. In section II we outline the mesic-nucleus theory to be used in the analysis. Detailed analysis is given in section III, and our findings are summarized in section IV.

## II. OUTLINE OF THE MESIC-NUCLEUS THEORY

The eigenvalue equation of the bound-state of an  $\eta$  meson in a nucleus is  $(H_0 + V)|\psi\rangle = \mathcal{E}|\psi\rangle$ . The  $\eta$ -nucleus potential  $V$  is complex because the  $\eta \rightarrow \pi$  channels are open. Hence, the eigenenergy  $\mathcal{E}$  is also complex and can be written as  $\mathcal{E} = E_{bd} - i\Gamma/2$ , where  $E_{bd}$  ( $< 0$ ) and  $\Gamma$  are the binding energy and width of the bound state, respectively. The momentum-space matrix elements of the leading-order potential are given by [19]-[20]

$$\langle \vec{k}' | V | \vec{k} \rangle = \langle \vec{\kappa}' | t_{\eta N}(W) | \vec{\kappa} \rangle F(\vec{k}' - \vec{k}), \quad (1)$$

where  $\vec{k}$  and  $\vec{k}'$  denote the initial and final  $\eta$  momenta in the  $\eta$ -nucleus c.m. frame and  $F(\vec{k}' - \vec{k})$  is the nuclear form factor. The  $t_{\eta N}$  is the operator for the scattering of  $\eta$  from the nucleon. The variables  $\vec{\kappa}$ ,  $\vec{\kappa}'$ , and  $W$  are, respectively, the initial and final  $\eta$ N relative

momenta, and the total energy of the  $\eta$ N system in its c.m. frame.

Without loss of generality, we use the coupled-channel isobar (CCI) model of Bhalerao and Liu [21] to calculate the potential given by Eq.(1). The reason for this is two-fold. First, we have at our disposal the detailed energy dependence of the model which reproduces remarkably the observable ( $\pi$ N  $S_{11}$  phase shifts) in the entire energy region where the nuclear binding of an  $\eta$  could take place. Second, it was this model that was used to predict the existence of  $\eta$ -nucleus bound states. Furthermore, as has been noted in the previous section, the discrepancy between the theoretical and experimental value of  $R$  exists for all published models, including the CCI model. Hence, we believe the general features of our findings are not limited to the model used.

In the CCI model of Ref.[21],

$$\langle \vec{\kappa}' | t_{\eta N}(W) | \vec{\kappa} \rangle = K \sum_{\ell} v_{\ell}(\vec{\kappa}', \Lambda_{\ell}) \mathcal{A}_{\ell}(W) v_{\ell}(\vec{\kappa}, \Lambda_{\ell}), \quad (2)$$

where  $K$  is a kinematic factor and  $\ell = 0, 1, 2$  are, respectively, the  $s$ -,  $p$ -, and  $d$ -wave  $\eta$ N interactions. The  $v_{\ell}$  are off-shell form factors of range  $\Lambda_{\ell}$ , and  $\mathcal{A}_{\ell}$  are the energy-dependent amplitudes. For bound-state problems,  $p$ - and  $d$ -wave interactions have negligible contributions. Consequently, we will only consider the  $s$ -wave  $\eta$ N interaction and omit the subscript  $\ell$ . The amplitude  $\mathcal{A}$  is given by

$$\mathcal{A}(W) = \frac{g^2}{2WD(W)}. \quad (3)$$

Conversely, if  $\tilde{\mathcal{A}}$  is the amplitude that gives the measured  $E_{bd}$  and  $\Gamma/2$ , then Eq.(3) can be used to derive the energy dependence of the denominator, namely,

$$D(W) = \frac{g^2}{2W\tilde{\mathcal{A}}}. \quad (4)$$

In the above equations  $g$  is the  $\eta$ NN\* coupling constant. Here, N\* is the  $s$ -wave isobar N\*(1535) which has a mass between 1525 and 1545 MeV and a Breit-Wigner width from 125 to 175 MeV [22]. For mesic-nucleus calculations,

$$W = m_{\eta} + m_N + \langle B_N \rangle, \quad (5)$$

where  $\langle B_N \rangle < 0$  is the average binding energy of the nucleon. In Eq.(3)

$$D(W) = W - M_{N^*}(W), \quad (6)$$

and

$$M_{N^*}(W) = M^0 + r(W) + \mathcal{R}e[\Sigma^{med}(W)] + i \mathcal{I}m[\Sigma^{med}(W)], \quad (7)$$

with  $\Sigma^{med} = \Sigma^{free} + \Sigma^{abs}$ . The  $\Sigma^{free}$  is the  $N^*$  self-energy arising from its decays to the  $\eta N$ ,  $\pi N$ , and  $\pi\pi N$  channels in free space. If  $\gamma^{free}(W)$  denotes its total free-space decay width, then  $\frac{1}{2}\gamma^{free}(W) = -\mathcal{I}m[\Sigma^{free}(W)]$ . The bare mass  $M^0$ , coupling constant  $g$ , range parameter  $\Lambda$  needed for the calculation of  $\Sigma^{free}$  were determined from fitting the experimental  $\pi N$   $S_{11}$  phase shifts [21]. The  $\Sigma^{abs}$  is the  $N^*$  self-energy arising from true absorption (or annihilation) by nucleons of the pions coming from  $N^* \rightarrow \pi N$ , and  $\pi\pi N$  decays. To our knowledge, microscopic absorption model that can fit systematically all experimental data is still not available. In the literature,  $\mathcal{I}m[\Sigma^{abs}]$  has been estimated in the framework of local-density approximation, and  $\mathcal{R}e[\Sigma^{abs}]$  is treated as a parameter [23]. It was found that total  $-\mathcal{I}m[\Sigma^{abs}] \simeq 35$  MeV at  $W = 1535$  MeV and at nuclear density  $\rho = \rho_0 = 0.17 \text{ fm}^{-3}$ . We extend this result to the subthreshold region by using  $-\mathcal{I}m[\Sigma^{abs}] = 35(q/\tilde{q})^3(\rho/\rho_0)^2$  MeV. Here,  $\tilde{q}$  is the  $\pi N$  relative momentum at  $W = 1535$  MeV and  $q$  the corresponding one at  $W < (m_N + m_\eta)$ . The exponent of  $q$  is based on the local-density result [23] on the momentum dependence of  $\Sigma^{abs}$  while the exponent of  $\rho$  is based on the fact that in a nucleus, pion absorption involves at least two nucleons. In principle, any subthreshold  $N^*$ -nucleus interactions can contribute to the real part of the  $N^*$  self-energy. We denote these contributions collectively as  $r(W)$  in Eq.(7).

We emphasize that  $\mathcal{I}m[\Sigma^{abs}]$  has the same sign as  $\mathcal{I}m[\Sigma^{free}]$ , as required by the unitarity of an optical potential. Hence,  $|\mathcal{I}m[\Sigma^{med}]| \geq |\mathcal{I}m[\Sigma^{free}]|$ . The dependence of  $\Sigma^{free}$  and the maximal  $\Sigma^{med}$  on  $W$  are shown, respectively, as the dash-dotted and solid curves in fig.1. At any given  $W$ , a physically meaningful  $\mathcal{A}(W)$  must always yield an  $\mathcal{I}m[\Sigma^{med}]$  situated in the ‘‘physical zone’’ bordered by these two curves, which we term the unitarity requirement. In fig.1 the left and right vertical lines show the positions of  $W$  corresponding, respectively, to nucleon binding energies  $\langle B_N \rangle = -100$  and  $-30$  MeV. As one can see,

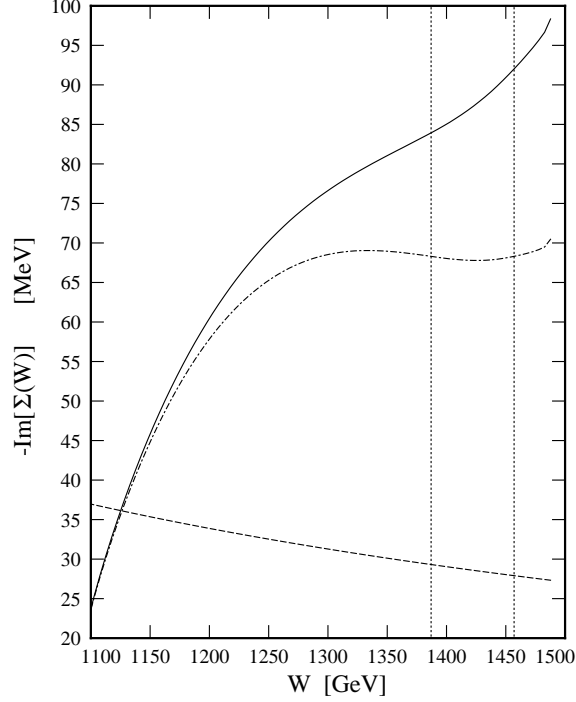


FIG. 1: The energy dependence of  $-\mathcal{I}m[\Sigma^{free}]$  (dash-dotted curve) and  $-\left(\mathcal{I}m[\Sigma^{free}] + \mathcal{I}m[\Sigma^{abs}]_{\rho=\rho_0}\right)$  (solid curve). The left and right vertical dotted lines indicate, respectively, the  $W$  corresponding to  $\langle B_N \rangle = -100$  and  $-30$  MeV. The dashed curve gives the energy dependence of  $-\mathcal{I}m[\Sigma^{med}]$  in case the experimental spectrum [17] is due solely to mesic-nucleus formation (see the text in Section III).

between these two  $\langle B_N \rangle$ 's the lower boundary of  $\mathcal{I}m[\Sigma^{med}]$  is nearly constant.

The quantity  $r + \mathcal{R}e[\Sigma^{abs}]$  in Eq.( 7) represents the real part of the  $N^*$ -nucleus interaction which we denote as  $V_{N^*}$ . Equation (7) can then be written as

$$M_{N^*}(W) = M^0 + V_{N^*}(W) + \mathcal{R}e[\Sigma^{free}(W)] + i \mathcal{I}m[\Sigma^{med}(W)] . \quad (8)$$

Using Eq.(8) in Eq.(6), we obtain

$$D(W) = W - \left( M^0 + V_{N^*}(W) + \mathcal{R}e[\Sigma^{free}(W)] + i \mathcal{I}m[\Sigma^{med}(W)] \right) . \quad (9)$$

Upon equating the real and imaginary parts of Eq.(9), one obtains

$$V_{N^*}(W) = W - \mathcal{M}(W) - \mathcal{R}e[D(W)], \quad (10)$$

and

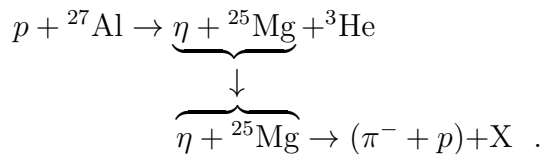
$$\mathcal{I}m[\Sigma^{med}(W)] = -\mathcal{I}m[D(W)]. \quad (11)$$

In Eq.(10),  $\mathcal{M}(W) \equiv M^0 + \mathcal{R}e[\Sigma^{free}(W)]$  and  $W$  is given by Eq.(5). We recall that  $\langle B_N \rangle$  is the average nucleon binding energy. Because the nucleons are bound,  $\langle B_N \rangle < 0$ . On the other hand,  $V_{N^*}$  can be either negative or positive, depending on whether the interaction is attractive or repulsive.

### III. ANALYSIS AND DISCUSSION

If the centroid of the experimental peak at  $-13$  MeV and half-width of  $5$  MeV are due solely to the formation of the  $\eta$ -mesic nucleus  $^{25}\text{Mg}_\eta$  via Process M, then an amplitude  $\tilde{\mathcal{A}} = -(0.0521 + 0.0099i) \text{ fm}^2$  is required to reproduce the above data. Upon using Eqs.(4) and (11) to solve for  $\mathcal{I}m[\Sigma^{med}(W)]$ , we obtain the dashed curve in fig.1. As one can see, this curve intersects the physical zone at  $W \simeq 1125$  MeV, which, by Eq.(5), corresponds to a  $\langle B_N \rangle \simeq -360$  MeV. This is clearly an unrealistic value which we regard as a strong indication that Process M alone is insufficient in describing the observed spectrum.

Indeed, the  $\eta$  produced in the intermediate state can also be scattered by the residual nucleus and emerge as a pion, without being first captured by the nucleus. We denote this multi-step reaction as Process S (S for scattering):



The essential portion of the reaction dynamics that differentiates the S and M processes, as indicated by upper and lower braces in the corresponding reaction equations, are illustrated in fig.2. We emphasize that because these two reaction paths lead to the same measured final state, they cannot be distinguished by the experiment. Consequently, in theoretical analysis one must take coherent summation of the two amplitudes to account for the

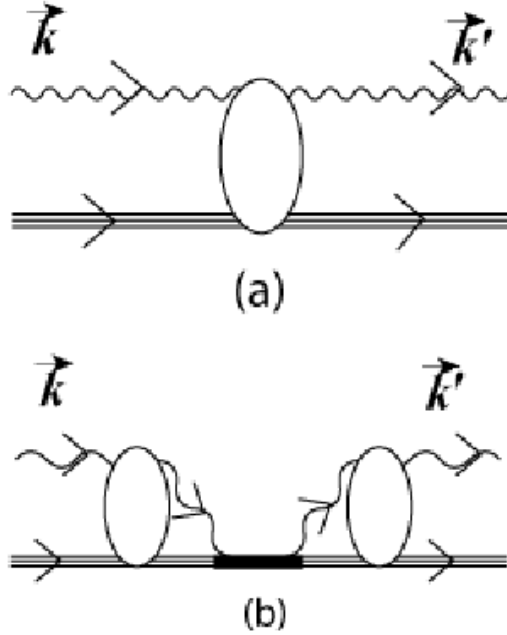


FIG. 2: (a) Reaction diagram of  $f_s$ . (b) Reaction diagram of  $f_M$ . The wavy and multiple lines represent, respectively, the  $\eta$  and  $^{25}\text{Mg}$ . The open oval denotes the  $\eta$ -nucleus interaction  $V$ . The filled line in (b) denotes the mesic nucleus.

quantum interference between them. We, therefore, fit the experimental spectrum by using the sum of two amplitudes:

$$\alpha |f_s + f_M|^2 = \alpha \left| \langle \vec{k}' | V(E) | \vec{k} \rangle + \frac{\langle \vec{k}' | V(E) | \psi \rangle \langle \Psi | V(E) | \vec{k} \rangle}{E - (E_{bd} - i\Gamma/2)} \right|^2, \quad (12)$$

where  $V$  is given by Eq.(1),  $E \equiv W - m_\eta - m_N - \langle B_N \rangle$ ,  $\psi$  is the wave function of bound  $\eta$ , and  $\Psi$  is its adjoint [24]. We have noted that in the threshold and subthreshold regions,  $\eta$ -nucleus interaction is isotropic and that the matrix elements  $\langle k' | V(E) | k \rangle$  are nearly constant for  $k$  and  $k'$  between 0 and 100 MeV/c. Because of these aspects of the  $\eta$ -nucleus interaction and the experimental selection of events corresponding to  $\eta$  being produced nearly at rest, Eq.(12) can be evaluated at  $|\vec{k}| = |\vec{k}'| \simeq 0$ .

One should note that in Eq.(12), there is only one parameter  $\alpha$  and its role is to just adjust the overall magnitude. We emphasize that we used the same  $V$  in calculating  $f_s$  and



$f_M$ , and that the values of  $E_{bd}$  and  $\Gamma/2$  obtained with this  $V$  were kept fixed during the fit. Furthermore, we square the sum of the amplitudes, in marked contrast to using the sum of the squared individual amplitudes. Hence, interference effects between the amplitudes are present in our analysis while they are absent in the COSY-GEM fit.

Our main goal is to find answer to the following questions: (1) Would it be possible to explain the spectrum by having  $|E_{bd}| \ll 13$  MeV in  $f_M$ ? (2) Is  $V_{N^*}$  attractive or repulsive?

In our previous work [19], we predicted the existence of  $\eta$ -mesic nuclei with  $\langle B_N \rangle = -30$  MeV, but without the inclusion of  $N^*$ -nucleus interaction. In other words, we have set both  $V_{N^*}$  and  $\mathcal{I}m[\Sigma^{abs}]$  equal to zero. The use of average nucleon binding energy  $\langle B_N \rangle = -30$  MeV is based on the findings from various studies of meson-nucleus scattering [25, 26]. Applying the same approach to  $^{25}\text{Mg}$ , we obtained  $\mathcal{E} = E_{bd} - i\Gamma/2 = -(6.5 + 7.1i)$  MeV. Upon using this  $\mathcal{E}$  and the corresponding  $V$  to calculate  $f_M$  and  $f_S$ , we obtained the result given in row (a) of table I and the spectrum is displayed as the dotted curve in fig.3. As one can see, the peak position of this curve appears at  $-10.5$  MeV. This 4.0-MeV downward shift from  $-6.5$  MeV indicates clearly the importance of interference effect. With the use of  $V$  obtained with  $V_{N^*} = -24$  MeV and  $-\mathcal{I}m[\Sigma^{abs}] = 0.65$  MeV, we obtained  $E_{bd} = -8.0$  MeV and  $\Gamma/2 = 9.8$  MeV. The corresponding spectrum given by Eq.(12) is shown as solid curve in fig.3. The peak position of this curve is at  $-12.5$  MeV, which agrees with the COSY-GEM result of  $(-13.13 \pm 1.64)$  MeV. The quantitative aspect of this latter calculation is given in row (b) of table I.

It is interesting to note from table I that fits (a) and (b) give same value to the overall conversion parameter  $\alpha$ . As indicated in section II, the  $\eta$ -nucleus interaction strength is given by  $D(W)$  and its values are shown in the 6th and 7th columns of the table. The comparison of the 7th and 8th columns of the table shows that  $\mathcal{I}m[D](\equiv -\mathcal{I}m[\Sigma^{med}]) \geq -\mathcal{I}m[\Sigma^{free}]$ . Hence, they satisfy the unitarity requirement. We also did calculations using larger  $\mathcal{I}m[D]$ . However, they led to larger calculated half-widths which worsened the fit. Consequently, we conclude that the present data require  $\mathcal{I}m[\Sigma^{med}]$  being close to the lower boundary of the physical zone of the self-energy (the dashed-dotted curve in fig.1). This in turn implies that in the recoilless transfer reaction of Ref.[17],  $\mathcal{I}m[\Sigma^{abs}] (= \mathcal{I}m[\Sigma^{med}] - \mathcal{I}m[\Sigma^{free}])$  is

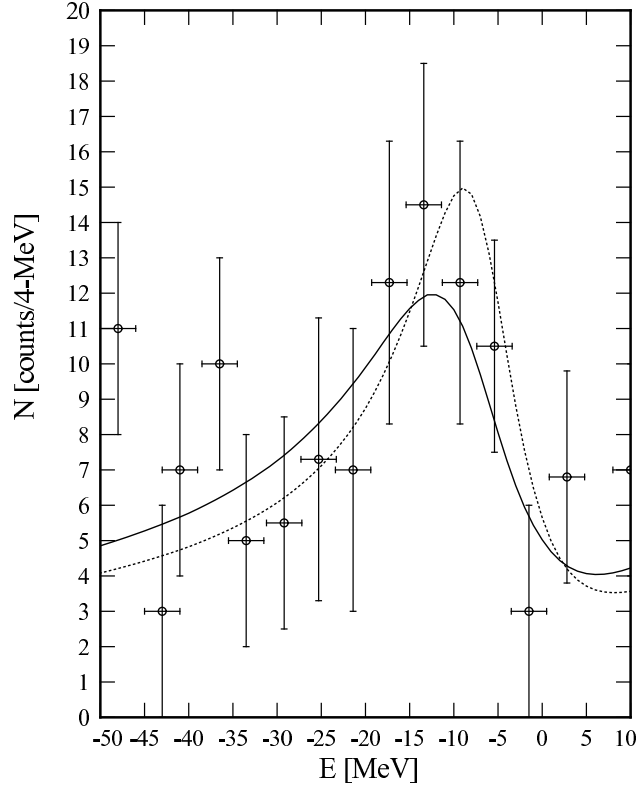


FIG. 3: Spectra obtained with (a) potential  $V$  giving  $E_{bd} - i\Gamma/2 = -(6.5 + 7.1i)$  MeV (dashed curve), and (b) potential  $V$  giving  $E_{bd} - i\Gamma/2 = -(8.0 + 9.8i)$  MeV (solid curve). The data are from Ref.[17].

TABLE I: Quantitative details ( $\alpha$  is in counts/fm<sup>2</sup>; all other quantities are in MeV).

Fit	$\alpha$	$E_{bd}$	$\Gamma/2$	$\langle B_N \rangle$	$\mathcal{R}e[D]$	$\mathcal{I}m[D]$	$-\mathcal{I}m[\Sigma^{free}]$	$\mathcal{M}$	$V_{N^*}$
(a)	4.2	-6.5	7.1	-30	-164	68.3	68.3	1622	0
(b)	4.2	-8.0	9.6	-30	-140	69.0	68.3	1622	-24

very small, and pion absorption takes place mainly in the nuclear surface region where the condition  $\rho/\rho_0 \ll 1$  leads to a very small  $\mathcal{I}m[\Sigma^{abs}]$ .

## IV. CONCLUSIONS

Our analysis shows that two reaction processes are contributing to the observed spectrum of the bound  $\eta$  in  $^{25}\text{Mg}$ . The interference between these processes causes the centroid of the observed spectrum to appear at an energy stronger than the actual binding energy of the  $\eta$  meson. The effective  $\eta\text{N}$  scattering lengths that reproduced  $E_{bd}$  and  $\Gamma/2$  used in  $f_M$  associated with the dashed and solid curves of fig.3 are, respectively,  $(0.226 + 0.094i)$  fm and  $(0.250 + 0.123i)$  fm. The corresponding imaginary-to-real part ratios are  $R=0.42$  and  $0.49$ , consistent with theories (see Section I). We, therefore, explained the apparent discrepancy between theory and experiment.

The present analysis also indicates that the real part of the interaction between  $\text{N}^*$  and  $^{25}\text{Mg}$  is attractive at energies below the  $\eta\text{N}$  threshold. This latter new nuclear information should be of value to nuclear physics studies involving the baryon resonance  $\text{N}^*(1535)$  in medium-mass nucleus, such as  $^{25}\text{Mg}$ .

We emphasize that the existence of S and M processes and the interference between them are of a general nature. Consequently, our finding on the effects arising from this aspect of reaction dynamics is model-independent. On the other hand, while the specific value of  $V_{\text{N}^*}$  may be model-dependent, its sign (or the attractive nature of the interaction) is model-independent. This is because the negative sign is required to provide more binding which, when combined with interference effects, can lead to sufficient downward shift of the peak in the binding-energy spectrum. We invite other researchers having at their disposal the detailed off-shell properties of their models to analyze the COSY-GEM data to further pin down the value of  $V_{\text{N}^*}$ .

- 
- [1] Q. Haider and L.C. Liu, Phys. Lett. **B172**, 257 (1986); **B174**, 465E (1986).
  - [2] M. Kohno and H. Tanabe, Phys. Lett. **B231**, 219 (1989); Nucl. Phys. **A519**, 755 (1990).
  - [3] M. Arima, K. Shimin, and K. Yazaki, Nucl. Phys. **A543**, 613 (1992).
  - [4] C. Wilkin, Phys. Rev. C **47**, R938 (1993).

- [5] L. Tiator, C. Bennhold, and S. Kamalov, Nucl. Phys. **A580**, 455 (1994).
- [6] N. Kaiser, P.B. Siegel, and W. Weise, Phys. Lett. **B362**, 23 (1995).
- [7] M. Batinić, I. Slaus, A. Svarc, and B.M.K. Nefkens, Phys. Rev. C **51**, 2310 (1995).
- [8] M. Batinić, I. Slaus, and A. Svarc, Phys. Rev. C **52**, 2188 (1995).
- [9] T. Waas and W. Weise, Nucl. Phys. **A625**, 287 (1997).
- [10] A.M. Green and S. Wycech, Phys. Rev. C **55**, R2167 (1997); **60**, 035208 (1999).
- [11] S. Garcia-Recio, T. Inoue, and E. Oset, Phys. Lett. **B550**, 47 (2002).
- [12] T. Inoue and E. Oset, Nucl. Phys. **A710**, 354 (2002).
- [13] H. Nagahiro, D. Jido, and S. Hirenzaki, Phys. Rev. C **68**, 035205 (2003); Nucl. Phys. **A761**, 92 (2005).
- [14] H. Nagahiro, M. Takizawa, and S. Hirenzaki, Phys. Rev. C **74**, 045203 (2006).
- [15] N.G. Kelkar, K.P. Khemchandani, and B.K. Jain, J. Phys. G: Nucl. Part. Phys. **32**, 1157 (2006).
- [16] C. Wilkin *et al.*, Phys. Lett. **B654**, 92 (2007).
- [17] A. Budzanowski *et al.*, Phys. Rev. C **79**. 012201(R) (2009).
- [18] M.G. Betigeri *et al.*, Nucl. Instr. Meth. Phys. Res. **A578**, 198 (2007).
- [19] Q. Haider and L.C. Liu, Phys. Rev. C **66** 045208 (2002).
- [20] Quamrul Haider and Lon-chang Liu, Acta Phys. Pol. (Conference Supplement) **B2**, 121 (2009).
- [21] R.S. Bhalerao and L.C. Liu, Phys. Rev. Lett. **54**, 865 (1985).
- [22] C. Amsler *et al.*, Phys. Lett. B **667**, 1080 (2008).
- [23] H.C. Chiang, E. Oset, and L.C. Liu, Phys. Rev. C **44**, 738 (1991).
- [24] L.S. Rodberg and R.M. Thaler, *Introduction to Quantum Theory of Scattering*, Academic Press (N.Y. 1967), pp.120-121.
- [25] L.C. Liu and C.M. Shakin, Phys. Rev. C **16**, 1963 (1977), see Appendix A.
- [26] W.B. Cottingham and D.B. Holtkamp, Phys. Rev. Lett. **45**, 1828 (1980).